Received: 28 September 2021 | Revised: 28 April 2023 | Accepted: 11 January 2024

DOI: 10.1049/rpg2.12950

IET Renewable Power Generation

The Institution of Engineering and Technology WILEY

ORIGINAL RESEARCH

Frequency control in an isolated wind-diesel hybrid system with energy storage and an irrigation water supply system

José Luis Monroy-Morales[1] | Rafael Peña-Alzola[2] | Rafael Sebastián-Fernández[3] | David Campos-Gaona[2] | Jerónimo Quesada Castellano[4] | José L. Guardado[1]

[1]Electrical Engineering, TecNM/Instituto Tecnológico de Morelia, Morelia, Mexico

[2]Electronic and Electrical Engineering, University of Strathclyde, Glasgow, UK

[3]Department of Electrical, Electronic and Control Engineering, UNED, Madrid, Spain

[4]Electronic Technology, University of the Basque Country, Vitoria, Spain

Correspondence
Rafael Peña-Alzola, Electronic and Electrical Engineering, University of Strathclyde, 204 George St., G1 1XW Glasgow, UK.
Email: rafael.pena-alzola@strath.ac.uk

Abstract

Wind-Diesel Hybrid Systems (WDHSs) integrate wind turbines into diesel power systems, reducing costs and emissions in isolated grids. Due to the no-load consumption of the Diesel Generators (DGs), fuel savings are only possible when the DGs are shut down. This requires a proper implementation of the frequency control to avoid perturbations because of the wind speed variations. During wind-only (WO) operation, the Synchronous Machine (SM) generates the isolated grid voltage and the frequency controller varies the energy stored/supplied by an Energy Storage System and consumed by the controllable loads to balance the power. In this paper, a Battery-based Energy Storage System (BESS) uses Li-Ion batteries with a Dual Active Bridge (DAB) and a grid-tie inverter connected to the isolated network. The controllable load is an Irrigation Water Supply System (IWSS), consisting of a pump supplying water to a reservoir tank. The pump is driven by a variable speed drive that uses a Permanent Magnet Synchronous Motor (PMSM). The coordinated control of BESS and IWSS gives full priority to the BESS for harnessing the wind potential whereas the IWSS consumes the excess of wind power. The full Wind Diesel Power System (WDPS) is modelled and simulated to validate the proposed system for different case scenarios.

1 | INTRODUCTION

An isolated Wind-Diesel Hybrid System (WDHS) integrates wind turbines (WTGs) with DGs to achieve maximum contribution from the wind resource and supply continuous, high-quality electrical power [1, 2]. These systems are used to generate electricity autonomously in areas without connection to the main grid. The DGs guarantees the power supply during periods of no wind. The main objective of WDPS is reducing fuel consumption to decrease operating costs and environmental consequences. A WDPS can operate in: diesel-only mode (DO), wind-diesel (WD) or hybrid mode, and wind-only mode (WO) also known as off-diesel mode [3]. In the operation mode DO, all the active and reactive power required in the isolated system is provided by the DGs with the WTGs being disconnected; this behaviour of the WDPS is that of a typical diesel power plant. The speed governors and load-sharing units of the DGs regulate the system frequency. The automatic voltage regulators (AVRs) in the SMs regulate the voltage amplitude. During WD operation, the WTGs generate active power that can be regarded as a negative load.

In the WO operation mode, the DGs are shut down and the only power generation is from the WTGs. A WDPS with the capability to operate in WO mode is said to be a high penetration WDPS (HP-WDPS) [4]. The fuel-saving is maximum because DGs consume fuel even with no-load (up to 40% in conventional equipment). Hence, reducing the power demand of the DGs by incorporating WTs to the WDPS does not translate into a significant reduction of the fuel consumption [4] and the WDPS must be capable of working with the DGs shut down during the periods of high wind availability. For this aim, the HP-WDPS requires additional components to achieve a proper frequency as will be explained later in the following sections.

Then energy storage system (ESS) can balance the intermittent wind power in an HP-WDPS [5] as the ESS can store surplus power from the wind turbines in periods of high wind speed and can generate power when wind speed is low [6, 7]. Furthermore, an ESS is a leading solution in ensuring power system quality and voltage stability [8]. There are many energy storage systems available such as batteries, supercapacitors, pumped hydro, flywheels, hydrogen storage, and compressed-air [9]. Batteries are a dominant and mature technology for the integration of ESSs into the electrical system with increased efficiency and decreasing costs. Lithium-ion batteries offer many advantages over other technologies such as high energy density, high load capability, long lifetime and reasonably short charge times. Lithium-ion batteries also present a high retention charge and low self-discharge (less than half that of NiCd and NiMH) [10, 11]. Power electronic converters enable the bidirectional power flow between the isolated grid and the battery.

Previous papers on wind-diesel systems consider Battery Energy Storage Systems (BESS) connected to the grid via an inverter that requires a line-frequency transformer [12–14]. This transformer is often bulky and can take up a large amount of space. To regulate power flow between the DC-link and the batteries, a bidirectional buck-boost converter may also be necessary.

However, in this paper considers an ESS that utilises a full-bridge grid-tie converter that is directly connected to the isolated network, and a dual active bridge (DAB) is used to provide galvanic isolation. The DAB is able to achieve zero voltage switching (ZVS), resulting in high efficiency levels (>98%). Additionally, this configuration uses a medium frequency transformer that is compact and has a small footprint. The DAB regulates the DC-link voltage, while the grid-tie inverter regulates the active and reactive power exchanged with the isolated grid. The advantages over traditional BESS configurations are quantified in references [15, 16], which refer only to the aspects related to power electronics.

The isolated wind-powered water supply drive utilizes a back-to-back converter to achieve optimal power quality and increased efficiency when operating at variable speeds. The use of variable speed drivers for pumps is enabled but the decreasing costs of power electronic converters based on IGBT or new SiC MOSFET. In isolated systems, it is crucial to minimize the harmonic content in power converters to prevent voltage distortion. To achieve this, an active rectifier was used in place of a diode-based converter without requiring large grid filters. This also enables the utilisation of film capacitors instead of electrolytic capacitors and increase the overall reliability of the ensemble [17].

Compared to a constant speed motor directly connected to the grid and a flow control valve the variable speed drive offers better efficiency. The energy savings are explained because, as per the affinity laws, brake horsepower varies with the cube of centrifugal pump speed and reducing pump speed reduces the pressure imparted to the fluid, decreasing the power consumption [18]. In addition, there are decreased fugitive emissions by eliminating the control valve and the associated piping. Finally, the variable speed drive (VSD) can be programmed to soft-start and soft-stop the process, eliminating hammer and reducing wear on mechanical components.

The variable speed driver also allows achieving faster dynamics for different flow rates, making possible the use of the irrigation system as controllable load in the overall control of the wind-diesel system. The grid-tie inverter has a unity power factor and is responsible for regulating the DC-link voltage, while the motor-side inverter regulates power consumption by varying the electric torque so that it works as a highly controllable load.

Power electronic converters have a fast response time that results in better dynamic response and power quality.

Controllable loads are used to consume the power excess from the wind turbine, which cannot be stored because the maximum power capability in the BESS has been reached or because the BESS is fully charged. In order to increase the overall efficiency, the controllable loads are not used merely for regulation but for useful purposes for example heating the DGs, desalinisation or pumping irrigation water. This paper considers the case of an Irrigation Water Supply System (IWSS), which consists of a centrifugal pump supplying water to a reservoir tank. The pump is driven by a variable speed drive, which comprises a permanent magnet synchronous motor and a back-to-back three-phase converter.

The WDPS presented in this paper consists of a DG, a WTG, an ESS based on lithium-ion batteries, an IWSS, and consumer loads as illustrated in Figure 1. The paper considers a wind-diesel power system working in wind-only operation mode and provides detailed models of all components, including electrical machines and power electronics, as isolated systems. Due to the low inertia, the interactions between components require detailed simulations. To measure the system frequency, a PLL is used instead of relying on the speed measurement from the SM encoder. This is analogous to sensorless control in motors, and simulation results demonstrate a satisfactory dynamic response suitable for frequency control. The primary contributions of the paper are:

- The selection process for the frequency controller gains in the wind-only (WO) mode is justified by the symmetrical optimum criterion, supplemented by engineering judgement for the final tuning. In contrast to prior methods that relied on trial and error iterations without any theoretical rationale, this approach is grounded in sound engineering principles.
- In the proposed frequency controller for the Wind Only (WO) operation mode, the State of Charge (SOC) limits are taken into account. This ensures effective power-sharing between the Battery-based Energy Storage System (BESS) and the Irrigation Water Supply System (IWSS), which functions as a controllable load. When the SOC is between 10% and 95%, the surplus wind power is used to charge the BESS, and during low wind speed periods, the BESS can supply the power deficit. The BESS is given priority, and the excess wind power is only utilized by the IWSS once the BESS reaches its maximum charging rate. If the SOC reaches 95%, and excess wind power is still present, the BESS cannot store any more excess power, and the IWSS load begins to consume active power. Conversely, when the SOC drops as low as 10%, the

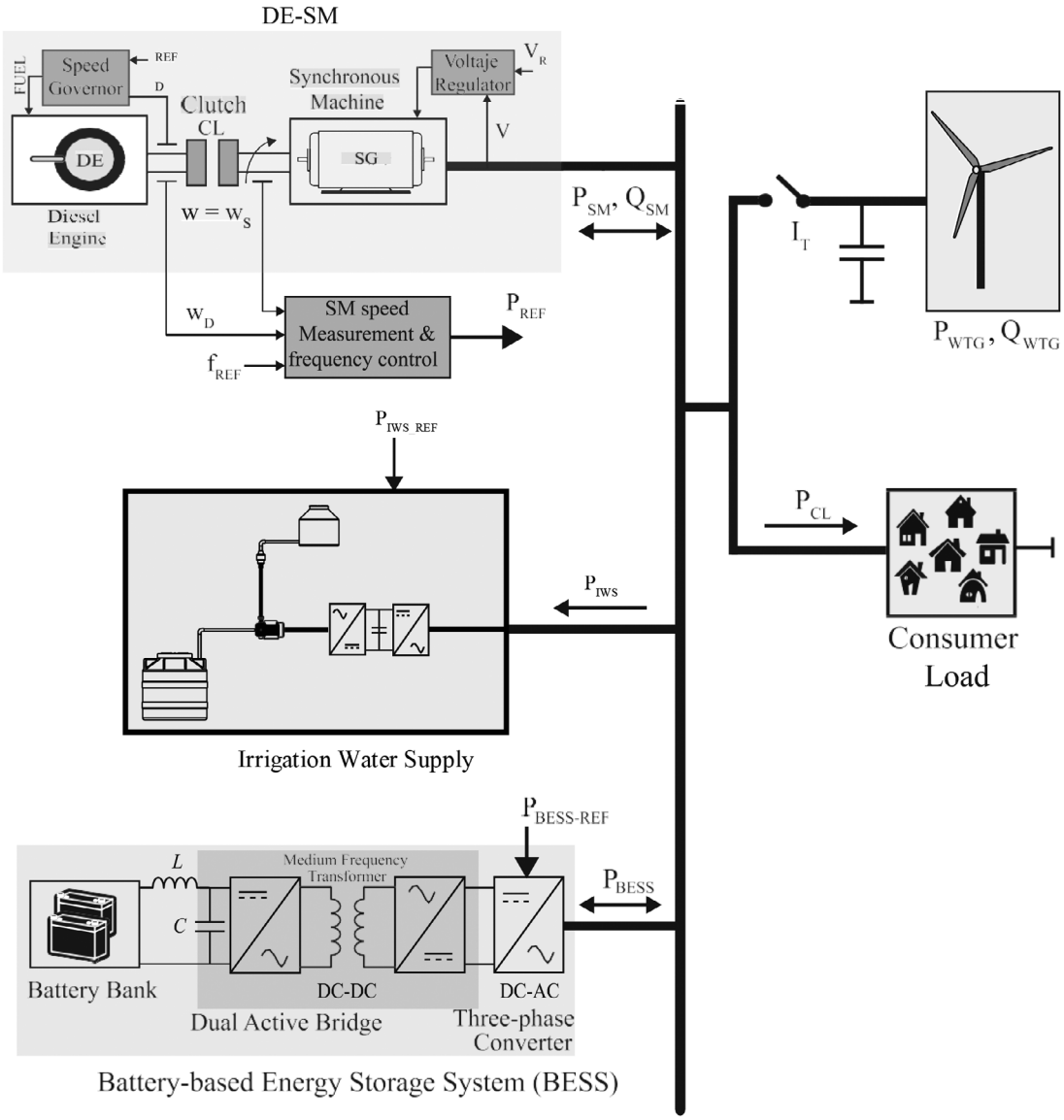

FIGURE 1 Overall diagram for the Wind-Diesel Hybrid System.

BESS is unable to provide the power deficit during low wind speed periods. In this event, if a frequency drop occurs and persists, the wind-diesel system must switch to wind-diesel operation mode.

- As power electronic converters become more standardized and their costs decline, variable speed drivers are increasingly being used for pumps. This paper focuses on pumps utilized in the IWSS, which incorporate back-to-back converters to improve power quality and increase efficiency under variable speed conditions. To prevent voltage distortion, it is essential to minimize harmonic content in the power converters connected to isolated systems. Accordingly, an active rectifier is employed rather than a diode-based converter. The variable speed drive delivers superior efficiency and faster dynamics for different flow rates compared to a constant speed motor connected directly to the grid and a flow control valve. The grid-tie inverter ensures a unity power factor and regulates the DC-link voltage, while the motor-side inverter regulates power consumption by adjusting the electric torque.
- Typically, the BESS is linked to the grid using an inverter through a line-frequency transformer, which can be bulky and require a lot of space. If the voltage levels differ considerably, a bidirectional buck-boost converter may be used to regulate power flow between the DC-link and the batteries [15, 16]. However, this paper adopts a different approach, utilizing a full-bridge grid-tie converter that is directly connected to the isolated network, alongside a dual active bridge (DAB) to provide galvanic isolation. The DAB can readily achieve zero voltage switching (ZVS), resulting in high efficiency (>98%). The utilization of a medium-frequency transformer in this configuration results in a smaller footprint and a more compact design. The DAB regulates the DC-link voltage, while

the grid-tie inverter regulates the active and reactive power exchanged with the isolated grid.

The proposed techniques utilize recent advancements in power electronics for wind-diesel systems to enhance their controllability and efficiency, resulting in better utilization of wind energy. There is potential for the development of wind-diesel systems in remote areas and islands in countries like Mexico, the United Kingdom, and Spain. The paper's proposals can aid in comprehending the overall control system and integrating power electronic interfaces.

After this introduction, Section 2 explains the modelling of the different elements in the HP-WDPS. Section 3 explains the frequency regulation of the isolated network. Section 4 explains in detail the overall control for the WO operation mode. Section 5 explains the simulation results for different case scenarios. Finally, Section 6 concludes the article.

2 | ISOLATED WDPS MODELLING

Wind power generation is subject to uncertainty due to atmospheric conditions. To maintain a constant system frequency corresponding to the synchronous machine speed, the power generated by the wind-diesel generator and wind turbines must be matched at all times by the power consumed by the consumer load and controllable loads. In the wind-diesel model, the wind power can be treated as a negative load, with the diesel generator supplying the power consumed by the loads minus the power generated by the wind turbines. Auxiliary loads must be of sufficient size to prevent negative loads at the diesel generator shaft, which could be dangerous. Simple resistor banks can serve as controllable loads and ensure the minimum load required by the diesel generator. These resistor banks are also used for heating purposes.

This situation should not persist indefinitely and the wind-diesel system should change its operation mode to wind-only. The reason for the change in the operation mode is that the fuel consumption in wind-diesel mode is not substantial. According to the Willans curve, the diesel generator consumes fuel even with no load [4]. The random nature of the wind power may cause numerous start/stop cycles in the diesel generator. The spectral distribution of the wind speed has a peak around minutes because of the turbulence. In order to reduce the number of start/stop cycles, an energy storage system (ESS) can be added to compensate for the lack/excess of wind power. During periods of low/high wind speed, the ESS will supply/absorb power to/from the system. The ESS should store enough energy to supply the consumer load for several minutes [19], which corresponds to the peak in the spectral density of the wind speed.

In terms of speed control and considering the frequency Equation (2), P_{WTG} and P_{CL} correspond to the wind power and the consumer load, respectively. Both powers are uncontrollable and random; P_{WTG} can be modelled statistically and P_{CL} can be modelled according to consumer habits. P_{WTG} and P_{CL} can be considered disturbances from a control point of view. P_{BESS} and P_{IWSS} are controllable and will be responsible for regulating the system frequency by balancing the active power generated and consumed in the system. The power references for the BESS and IWSS should match the consumer load minus the wind power to maintain a constant system frequency equal to its rated value. The BESS and IWSS should supply/absorb power with sufficient speed when compared to the consumer load and wind speed variations. This is the case as the power interface of the BESS and IWSS is based on power electronic converters with high switching frequency and high bandwidth.

The components forming the WDPS system are described below. The DG generates controllable active and reactive power. The WTG generates uncontrollable active power and consumes uncontrollable reactive power that depends on the random wind speed. The BESS and the IWSS can absorb controllable active power and only the BESS can provide controllable active power. The consumer load consumes uncontrollable active power (resistive loads), which depends on the demand requirements of the community and can be predicted based on the consumer's habits [19]. As the paper considers the system dynamics, sudden step changes in the consumer load are being applied. In practice, consumer load variations will never be as drastic and the load steps can be considered the worst-case scenario. Hence, this approach can be sufficiently representative to assess the dynamic response of the wind-diesel system. Similarly, steps in the wind speed are being considered instead of the gust models for evaluating the dynamic response against wind power variations.

The HP-WDPS uses an SM to produce the voltage waveform. The SM is part of the DG and engages to and disengages from the Diesel Engine (DE) by using a friction clutch. The WDPS operation mode is defined by the status of the clutch and the switch I_T for the WT shown in Figure 1. For the operation mode DO, the clutch is placed as engaged (CL = ON) and the switch for the WT is open (I_T = OFF), therefore, the DG generator supplies the power to the CL. In this mode, there is not sufficient wind speed (lower than the cut-in speed) and the WT cannot supply power. The BESS is idle except for supplying the trickle current that will guarantee the proper operation. Moreover, the BESS can be active during fast transients. The IWSS is only consuming the minimum power amount required for the irrigation availability. During WD operation, the switch for the WT is closed (I_T = ON), with the clutch remaining in its previous state, the DG generator supplies the power to the CL in combination with the WT. In this mode, there is sufficient wind speed (higher than the cut-in speed) so that the wind turbine can produce power. The WT behaves like a negative power and the fuel saving is not substantial. The reason for this is that the DG consumes power even with no load according to the Willans curve. The BESS can act for improving the dynamic response during fast transients because of wind gusts and changes in the CL. The IWSS is only consuming the minimum power amount required for irrigation availability. The switch for the WT is closed (I_T = ON) and the clutch is operating disengaged (CL = OFF) for the WO operation mode. In this WO operation mode, the DG generator is shut down and only the WT supplies the power

TABLE 1 Summary for the power flow of the different elements in the WDHS.

Operation mode	Diesel generator (DG)	Wind turbine (WT)	BESS	IWSS	Consumer Load (CL)
Diesel only	Generation	No generation	No storage	Minimum consumption	Consumption
Wind diesel	Generation	Generation	No storage	Minimum consumption	Consumption
Wind only	No generation	Generation	Storage in case of wind power excess	Minimum consumption and wind power excess	Consumption

TABLE 2 Different elements performing the frequency and voltage control.

Operation mode	Frequency control	Voltage control
Diesel only	DE speed governors	SG AVR
Wind diesel	DE speed governors	SG AVR
Wind only	BESS+IWSS	SG AVR (synchronous condenser)

to the CL. There is sufficient wind speed so that the wind turbine power is higher than the CL. The WO operation mode contributes to a substantial reduction in the fuel consumption of the wind-diesel system. The BESS stores the wind power excess (wind power minus CL) during periods of high wind speed. Conversely, the BESS supplies power to the CL (along with the WT) during periods of low wind speed. The IWSS consumes the minimum power amount required for the irrigation availability plus the wind power excess once the BESS have reached its power exchange limit or is fully charged. Table 1 summarises the power flow for the different elements of the wind-diesel system.

In DO and WD mode, the frequency control is performed by the speed governor of the Diesel Engine (DE). The speed governor regulates the diesel engine speed by providing an adequate amount of fuel to the pistons. The automatic voltage regulator (AVR) of the synchronous generator maintains the output voltage constant. This is achieved by varying the excitation voltage of the SG so that the necessary reactive power is supplied/consumed. In WO mode, the DE is disengaged from the SG that works as a synchronous condenser. The frequency regulation is performed by varying the power consumption with BESS and the controllable load IWSS. In WO mode, the voltage regulation is still carried out by the AVR of the synchronous condenser. Table 2 summarises the action of the different elements performing the frequency and voltage control.

2.1 | Wind turbine

In this paper is selected an asynchronous generator directly connected to grid as was characteristic of the fixed-speed wind-turbines. Fixed-speed asynchronous generators (FSAGs) are a prevalent choice for wind diesel systems, particularly in remote locations without access to the main grid, as evidenced in the literature [13]. The use of FSAGs offers several advantages, including:

- Cost-effectiveness relative to other wind energy technologies due to the simplicity of their design as an induction generator, requiring no power electronic converter and complex electronic controllers.
- This mature technology has been in use in the wind industry for several decades, resulting in lower costs.
- FSAGs also improve the stability of wind diesel systems, thanks to the damping effect of the inductor generation, where the torque is proportional to the slip.
- Additionally, FSAGs have a high conversion efficiency due to the lack of a power electronics interface and no slip rings, which wear out.
- The previous advantage results in a reliable wind turbine with ease of maintenance requiring no special training.
- While FSAGs cannot modify the rotation speed at will as in doubly fed induction machines (DFIG) and type 4 wind turbines (full rated back-to-back converters) to maximize the wind energy capture, a simple configuration using two rotation speeds by pole changing results in sufficient optimization without technical complexity.

Therefore, FSAGs' low cost, robust construction, and reliability with simple maintenance are remarkable features for the remote locations of wind diesel power systems (WDPS).

The WT uses a gearbox and a squirrel-cage rotor Induction Generator (WTIG) with a rated power of 275 kVA. As can be seen in Figure 1, the required reactive power is provided locally by a capacitor bank of 25 kVA at the WTIG terminals.

The WT takes the energy from the wind to transformer it into mechanical power at the shaft, which in turn is converted to electrical power by the WTIG. The WT is modelled using a lookup table that relates the power at the shaft P_{T-MEC} with the wind speed (v_{speed}) and the mechanical speed ω_t. The speed range of the WTIG for power generation is very narrow, between 1 and 1.02 in per unit [20] and this is why this type of WT is said to have a constant speed. Hence, adjusting the rotational speed to maximise the wind power capture is not possible with this kind of WT.

Some WDPS use WTGs [21–24] that allow variable speed operation to maximise the capture of wind energy at the expense of requiring a power electronic converter. The Doubly-Fed Inductor Generator (DFIG) requires a fractional-power converter whereas the synchronous machine requires a full-power converter. The constant-speed fixed-pitch WT-WTIG has important advantages when being used in remote locations typical of WDPSs such as robust construction, economical, and uncomplicated maintenance. Indeed, this type of WTs does not

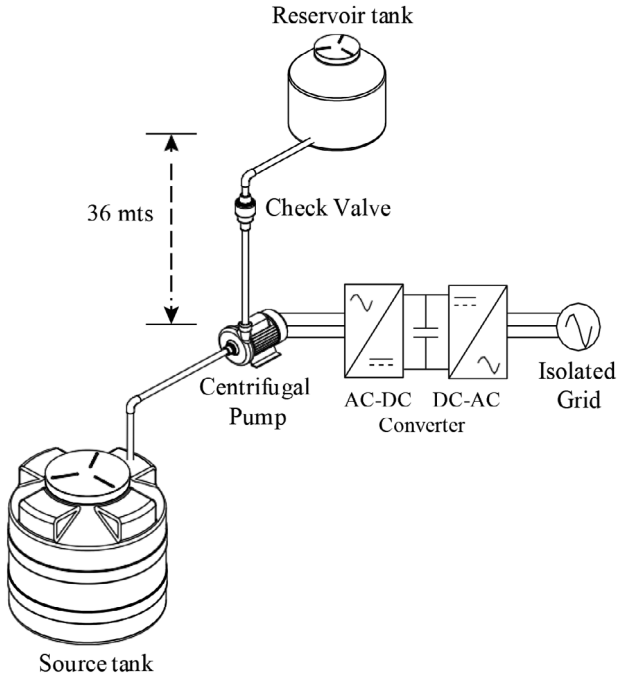

FIGURE 2 Irrigation water supply.

include either power electronic converters, which reduces the efficiency, or slip rings, which require periodic maintenance. Moreover, the wind power is proportional to the slip [25], which contributes to having a damped response in the system frequency [26, 27].

2.2 | Irrigation water supply system

The components of the IWSS are: a source tank, a pumping station, pipelines, a check valve and a reservoir tank. The irrigation water supply system was modelled as consisting of a constant load and controllable load. The constant load is the power required to guarantee a minimum amount of water in the reservoir tank by accounting for small leakages and evaporation. For the paper simulations, this value was set to 10 kW and it can be considered as another consumer load. The controllable load is used when there is a wind power excess and once the ESS is fully charged or has reached its maximum charging current (maximum power of the power electronic interface). The ESS covering the average load for minutes guarantees a reduction in the number of diesel starts [19]. The source tank is setting to 100 m^3 as the initial volume of water. The pumping station has a centrifugal pump located at floor level that pumps water to the reservoir tank located at 36 m. Both source tank and reservoir tank are modelled as a constant head tank block since they are large enough and can be assumed that the water level remains constant. The IWSS is shown in Figure 2, the pipelines connecting the tanks and the centrifugal pump which have a diameter of 20.84 cm with laminar friction constant for Darcy friction factor of 64. The centrifugal pump operates in a reference angular velocity of 1770 rpm with the head, speed and flow rate characteristic curves computed by using two one-dimensional table lookups. All these elements were modelled with Matlab/Simulink blocks of the library the Simscape Fluids [28].

The pumps are driven by a variable speed drive that uses a PMSM and a back-to-back converter as illustrated in Figure 2. The IWSS uses an active rectifier (instead of a passive diode bridge) in order to minimise the current harmonic injection that may affect the overall power quality in the isolated network. A full-bridge converter using vector control regulates the electrical torque and so the power because the speed variations are slow in comparison with the electrical time constant. Hence, the IWSS uses an interface completely based on power electronics converters and the power exchange can be easily regulated by the frequency control of the wind-diesel system. The selection of the motor for the variable speed drive present in the IWSS was based on efficiency. The BLDC motor is a feasible choice due to its high torque, robust construction, and low cost. However, it is well known that the BLDC motor torque has a higher ripple, which can lead to increased vibration and potentially affect the pump's reliability, especially during continuous operation. Moreover, PMSM motors have a higher efficiency than BLDC motors, especially at low loads. Therefore, the PMSM presents the best efficiency and the highest power density at the expense of higher cost because of the permanent magnets [29]. The selection of the IWSS motor is not critical and different options are available according to the efficiency, cost and reliability. Selecting an induction motor would have resulted in additional losses in the rotor and additional reactive power, but the motor is more inexpensive and reliable with no risk of demagnetisation. Alternatively, a synchronous reluctance motor could have been used, which can compete with the induction motor in terms of efficiency and is not as expensive as the PMSM [29]. All the mentioned machines use standard vector control with nested loops for the current and the speed with similar controller implementation. The PMSM used in this paper has two pole pairs ($p_p = 2$)) with a rated speed of 1800 rpm and a rated power of 450 kW. The variable speed drive uses voltage-oriented control in the grid-side converter and vector control in the motor-side converter as shown in Figure 3. The voltage-oriented control has an inner current loop for sinusoidal currents with unit power factor and the outer loop regulates the DC-link voltage, as illustrated in Figure 3(a). The vector control has an inner current control with a zero direct current for maximum torque per ampere in the PMSM and the outer loop is used to regulate the power consumed by the IWSS P_{IWSS} as shown in Figure 3(b). The control of P_{IWSS} uses an integral controller with a feed-forward component for fast dynamics. The feed-forward component considers that the consumed power $P_{IWSS} = T_e^* \cdot \omega_m$ is approximately equal to the electric reference torque T_e^* times the mechanical speed ω_m. This assumes negligible losses and slow variation of the mechanical speed when compared to the electrical magnitudes. The electric torque reference $T_e^* = 1.5 p_p \lambda i_q^*$ is varied quickly with the quadrature current i_q^* as shown in Figure 3(b) (λ is the permanent magnet flux). Because of the fast current control ($i_q^* \approx i_q$) and large speed time-constant that the power reference is approximately

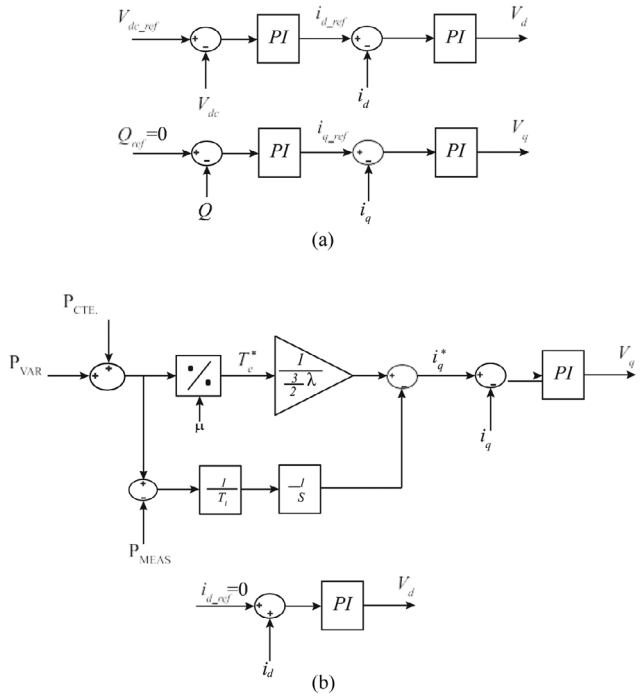

FIGURE 3 Block diagram of the variable speed drive used in the IWSS. (a) control of the grid-tie inverter; (b) control of the motor-side inverter.

the actual power consumed by the IWSS ($P_{IWSS} = 1.5p_p\lambda i_q^* \omega_m$). The losses are considered in the integral feedback controller, which will eliminate steady-state errors in the power reference.

Figure 3(b) shows that there is a constant power reference P_{CTE} for the minimum amount of continuous pumping water plus a variable power reference P_{VAR} varying with the wind energy availability. Hence, the IWSS can absorb the power surplus produced by the WTG to match the overall WDPS active power.

2.3 | Model of the battery energy storage

The BESS is conformed by a 236 V/142 Ah lithium-ion battery array along with a power electronic converter as illustrated in Figure 4. There are several reasons why Li-ion batteries are preferred over lead-acid batteries in wind-diesel hybrid systems [30–32]:

- Li-ion batteries are easier to dispose of when their lifetime is complete, as they do not contain heavy metals like lead, which can be hazardous to the environment and human health. This is especially important in remote locations where wind diesel systems are commonly used.
- In addition, Li-ion batteries have a longer cycle life and are better suited for irregular charging and discharging patterns, which reduces the logistics required for replacing batteries in remote locations. Li-ion batteries also have a higher energy density than lead-acid batteries, which results in a smaller footprint and lower weight, making them more practical for commissioning.
- Li-ion batteries can accept higher currents (C rate) than lead-acid batteries, which makes them more suitable for handling power variations resulting from wind-speed changes in isolated power systems. Furthermore, the variation in battery output voltage with depth of discharge is much smaller in Li-ion batteries than in lead-acid batteries, which makes it easier to design power electronics converters..
- Li-ion batteries can accept higher currents (C rate) than lead-acid batteries, which makes them more suitable for handling power variations resulting from wind-speed changes in isolated power systems. Furthermore, the variation in battery output voltage with depth of discharge is much smaller in Li-ion batteries than in lead-acid batteries, which makes it easier to design power electronics converters.
- While Li-ion batteries are more expensive than lead-acid batteries, their numerous advantages make them a preferred choice, and their cost is decreasing as they become a more mature technology.

The BESS is usually connected to the grid by using an inverter through a line-frequency transformer, which is bulky and presents a large footprint. A bidirectional buck-boost converter can also be present to regulate the power flow between the DC-link and the batteries [15, 16] if the voltages are much different. In this paper, the BESS uses a full-bridge grid-tie converter directly connected to the isolated network and a dual active bridge (DAB) for providing galvanic isolation. The DAB can easily achieve zero voltage switching (ZVS) so that the efficiency is high (>98%). This configuration uses a medium frequency transformer, which is compact and has a small footprint. This arrangement results in higher efficiency and lower size when compared to using line transformers for providing isolation and a buck-boost converter to connect different voltage levels [15, 16].

The bidirectional full-bridge converter enables the battery to be either charged or discharged according to WTG power availability. The switching frequency is 4 kHz and L-filters are used to limit the harmonic content of the grid current. The three-phase converter uses grid-voltage vector oriented control with nested loops as shown in Figures 5(a) and 5(b).

Figures 5(a) and 5(b) represent the active and reactive power, respectively.

The inner loops control the dq-currents whereas the outer loops control the active and reactive power. A Phase-Locked Loop (PLL) synchronises the dq-frame with the grid voltage vector. The d-current in phase with the grid voltage allows exchanging active power with the isolated grid whereas the q-current allows exchanging reactive power. The dq-current controllers are Proportional-Integral (PI) whereas the active and reactive power controllers are purely integral with feed-forward for fast dynamic response.

The DAB uses phase-shift modulation for controlling the power exchange between the battery and the DC-link capacitor. The DAB controller shown in Figure 5(c) is PI with the DC-link voltage error as input and the power reference as output. The phase shift angle is calculated with the following equation [33]:

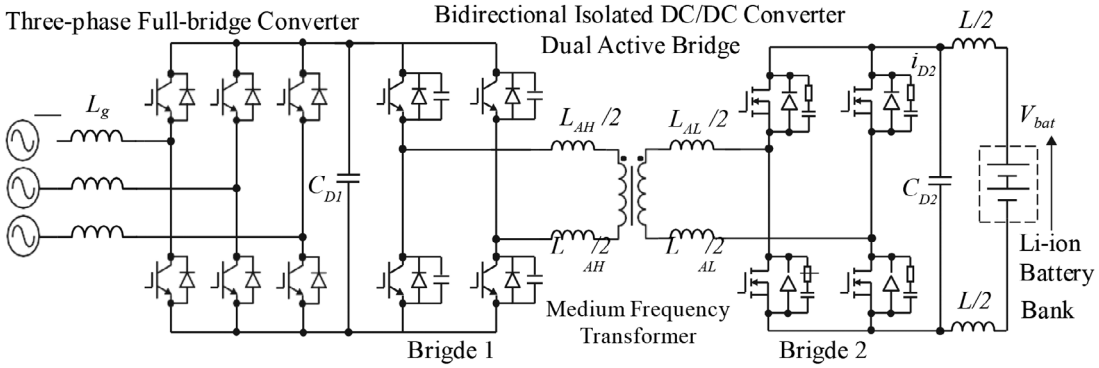

FIGURE 4 Components of the BESS comprising a three-phase full-bridge converter, a dual active bridge, and a battery bank.

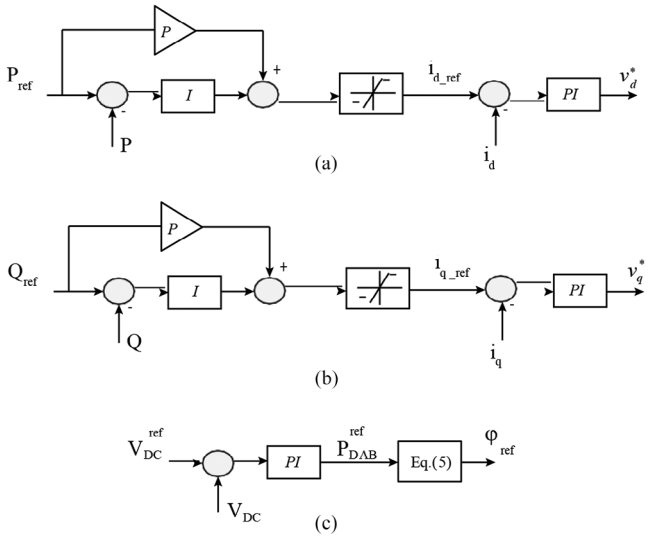

FIGURE 5 Control of the BESS three-phase converter.

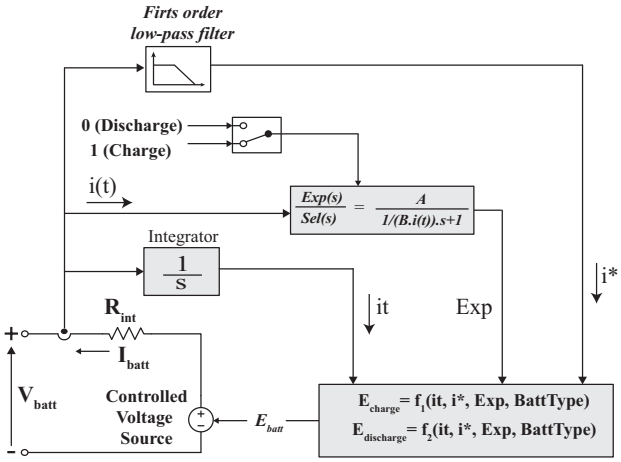

FIGURE 6 Equivalent circuit of the lithium-ion battery.

$$P_{DAB}^{ref} = \frac{nV_{bat}V_{dc}}{2\pi f_{sw}}\varphi_{ref}\left(1-\frac{\varphi_{ref}}{\pi}\right), \quad (1)$$

where P_{DAB}^{ref} is the power reference to the DAB, n the transformation ratio of the medium frequency transformer, V_{bat} the battery voltage, f_{sw} the switching frequency, and φ_{ref} the phase-shift reference angle. The transformation ratio $n = 4$ allows using a standard battery pack with 236 V for supplying the full-bridge DC-link voltage of 860 V. The switching frequency used in the DAB is 10 kHz. This provides an appropriate trade-off between efficiency and transformer size.

The lithium-ion battery is connected to the DAB DC-capacitor through an inductor (0.4 mH) to limit the battery's current ripple. The model for the lithium-ion battery used in Matlab/Simulink is shown in Figure 6 [34] and consists of a variable voltage source and internal resistance. The variable voltage source represents the internal voltage of the battery, which depends on the battery parameters and the SOC.

The addition of an ESS allows for the reduction of the number of start/stop cycles [19] in the DG, which contributes to improve the overall energy efficiency and to reduce the wear out. The ESS should store the required amount of energy to provide to the consumer load for several minutes corresponding to a peak in the spectral density of the wind speed. The 150 KW converter supplying the load for 10 min, with the battery SOC operating in 20% as minimum and 95% as maximum (0.75 pu) is used to calculate the energy stored in the BESS. Considering the previous, the reached total energy is 33.3 kWh and a battery capacity of 33.3 kWh/236 V = 142 Ah.

3 | CONTROL OF THE WDPS

In operation modes DO and WD, locking the friction clutch allows a full engagement of the DE and SM, regulating thus the frequency employing the DE speed governor. To obtain a constant frequency, the speed governor must maintain an immediate balance between the active powers produced and consumed in the isolated grid. The power of the SM during WD operation can be represented in the next equation as:

$$P_{DE} + P_{WTG} - P_{CL} \underbrace{-P_{BESS} - P_{IWSS}}_{-P_C} = J_s\omega\frac{d\omega}{dt}, \quad (2)$$

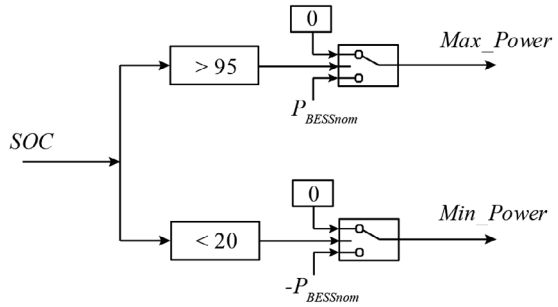

FIGURE 7 Maximum and minimum controllable power according to the battery SOC.

where the DE produces the P_{DE} power, P_{WTG} is the wind power from the WTG, P_{CL} is the power load P_{BESS} is the power absorbed or supplied by the BESS, P_{IWSS} is the power consumption of the IWSS, J_s is the overall inertia and ω the mechanical speed. P_{DE} and P_{WTG} are positive when producing active power and P_{IWSS} and P_{BESS} are positive when consuming active power. The controllable loads of the HP-WDPS P_C corresponds to P_{IWSS} plus P_{BESS}.

In steady state, the frequency must be constant with $\frac{d\omega}{dt} = 0$ and equal to its rated value. Equation (2) indicates that the diesel speed governor must order to produce the necessary power P_{DE} to match the power consumed by all the loads minus the power produced by the wind turbine.

In the operation modes DO and WD, the controllable power source/sink BESS and the controllable load IWSS only actuate to prevent the negative power in the DG for the case when the WTG generates an excess of wind power (higher than the consumer load). The power P_{DE} must be always positive to enable the speed governor to regulate frequency. The BESS absorbs and the IWSS consumes power so that P_{DE} is always a positive amount so that the speed governor can carry out the frequency regulation. In the case the negative power in the DG persists, the WO operation mode must be applied through the HP-WDPS overall control.

4 | WIND-ONLY MODE CONTROLLER

The active power for this mode of operation is produced only by the WTG since the SM is uncoupled from the DE. As P_{CL} and P_{WTG} are not controllable, the BESS and the IWSS must balance the wind power excess to achieve the speed regulation. The proposed controller for the WO operation mode considers the limits of the SOC battery to perform the power-sharing between the BESS and the IWSS.

In Figure 7, the maximum and minimum battery SOC limits are 95% and 20%, respectively. For SOC >95%, the battery is considered to be fully charged; it cannot absorb more wind excess power, but it can supply power to the loads. For SOC <20%, the battery is considered to be fully discharged; it cannot supply additional power to the loads, but it can absorb wind excess power. For 20% <SOC<95% the battery can

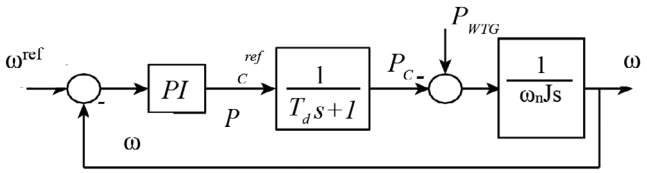

FIGURE 8 Frequency control with the synchronous condenser.

exchange power in both directions up to the nominal value of the three-phase converter ($\pm P_{BESS\_nom}$).

For the operation mode WO, a PI controller is used to regulate the frequency. Droop control is used to regulate the power output of multiple generators that are connected in parallel while supplying a common load. This ensures that each generator shares the load proportionally according to its capacity. In the wind-diesel system presented in the manuscript, droop control is not necessary since there is only one diesel generator. However, if there were multiple diesel generators, droop control or any other power-sharing technique would be necessary. Droop control (sharing units) is a common feature of the speed regulators and AVRs for diesel generator.

Regarding speed control with a PI controller to regulate the system frequency, there are several considerations to keep in mind. In overall frequency Equation (2) of the manuscript P_{DE} is zero because simulations are in wind-only mode. As mentioned in the previous paragraph P_{WTG} and P_{CL} are uncontrollable loads that can be considered disturbances from a control point of view. P_{BESS} and P_{IWSS} are controllable and will be responsible for regulating the system frequency by balancing the active power generated and consumed in the system. From the control point of view, P_{BESS} and P_{IWSS} are considered jointly as the controller output $P_C = P_{BESS} + P_{IWSS}$. For this case, a droop controller could also be considered as both the BESS and IWSS aim to regulate the frequency. However, the BESS has limits on the maximum power that it can supply and absorb once the battery is depleted and fully charged. In addition, the BESS should have priority in order to reduce the number of start/stop cycles in the diesel generator [19]. P_{IWSS} can only consume power and it is limited by the VSD rating.

The frequency regulator proposed in the manuscript consists in a PI controller. The frequency regulation will be isochronous (no steady-state error at different load consumption) because of the integrator. The controlled power P_C is the regulator output variable as illustrated in Figure 8. The controlled power P_C is shared between the BESS and IWSS. When the frequency fall, the system requires additional power and only the BESS can supply it. If there is an excess of wind power generation and the systems frequency increase, the BESS will have preference in dealing with the energy surplus. Once, the BESS has reached its full power rating or is fully charged, the IWSS will start consuming power by pumping water for the irrigation system. Moreover, the limitations in the output power of the BESS (which depends on the state of charge) and IWSS (unidirectional) are considered in the anti-windup mechanism of the PI controller as illustrated in Figure 9. The sharing scheme between BESS and IWSS for the controller output power is shown in Figure 10.

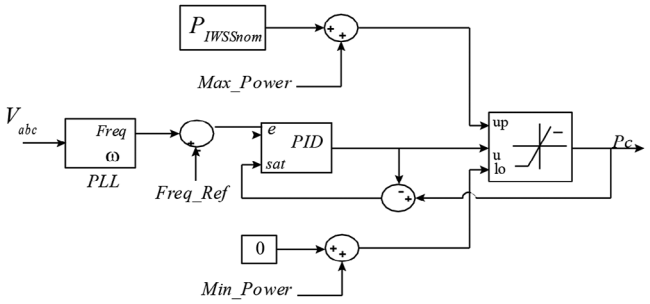

FIGURE 9 PI regulator for frequency control.

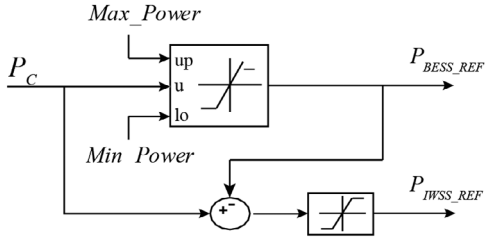

FIGURE 10 Control algorithm for the Power-Sharing between the BESS and the IWSS.

Considering the swing Equation (2) with $P_{DE} = 0$ (WO mode), the block diagram with the transfer function that relates the controllable power P_C (P_{BESS} and/or P_{IWSS}) and the SM speed ω is shown in Figure 8. The power P_{WTG} is considered a disturbance to be removed by the closed-loop control. The input of the PI controller is the speed error and the output is the power reference to the IWSS and/or the BESS. The time constant T_d corresponds to the response time of the power electronic converters of the BESS and IWSS.

The speed is not measured from the SM encoder; instead, the system frequency is estimated from the three-phase grid voltage by using a PLL. This is analogous to using a sensorless speed estimation [35] and simulations show that the dynamic response is sufficiently fast due to the slow time constant of the mechanical speed. The output limits of the PI controller (and its anti-windup mechanism) consider the power limits of the BESS and the availability of the IWSS as per Figure 9.

The plant of the frequency (speed) control corresponds to the swing Equation (2) and consists of a simple integrator. For this case, a proper tuning procedure for the PI controller in the symmetrical optimum criterion [36]. The proportional gain and the integration time should be adjusted as follows:

$$K_p = \frac{\omega_n J}{aT_d}, \tag{3a}$$

$$T_i = a^2 T_d, \tag{3b}$$

with $a = 3$ for triple-pole response [37] and ω_n the nominal pulsation. The value of the time constant T_d was selected to be 25 ms for a robust response. The proposed controller, shown in Figure 9, uses a PI whose output power reference is shared between the IWSS and the BESS.

In the power-sharing algorithm between the BESS and IWSS of Figure 10, the BESS has full priority in order to store the maximum energy in the periods of wind power excess. After the battery SOC reaches a value higher than 95%, the IWSS starts consuming the active power surplus that the battery is no longer able to store. After the battery SOC goes lower than 20%, the battery is fully discharged (without incurring deep discharge) with no capability to supply electricity to the loads. The frequency will drop and the overall control should order the DG to start producing power to avoid the system collapse by changing to the operational mode WD.

5 | SIMULATIONS RESULTS

The WDPS was simulated using MATLAB/Simulink [34] to verify the proposed features and to evaluate the proper operation. The simulations were based on Figure 1 in the operational mode WO with a 300 kVA SM, a 275 kVA WT, a 150 kW BESS and a 450 kW IWSS. The consumer load is initially 40 kW with positive and negative step changes of 50 kW during the tests. The simulations were carried out considering the SOC for three case studies: 95%, 50%, and 10%. These values are illustrative examples as the SOC will always remain between 20% and 95%. In each case, wind speed changes and consumer load variations were tested.

5.1 | Case SOC = 95%

For the case with SOC = 95%, the wind speed is initially 10 m/s, it increases up to 11 m/s at $t = 0.5$ s and finally, it decreases to 9 m/s at $t = 10$ s. The WTG generated power increases from 200 kW to 265 kW. The load consumption decreases from the initial value of 90 kW down to 40 kW at $t = 4$ s and later increases up to 90 kW at $t = 7$ s. These power variations are illustrated in Figure 11 considering positive power in both cases, when the WTG is supplying and when the consumer load is consuming.

Figure 12 shows P_{IWSS} and P_{BESS} when the WTG is generating excess active power. With SOC = 95%, the battery cannot store more energy and the proposed controller orders the dump load to consume the excess active power until $t = 10$ s when there is a negative step in the wind speed. After $t = 10$ s the IWSS load stops consuming power as there is no longer wind power excess. During the time range from $t = 4$ s to $t = 7$ s, the IWSS load increases the power consumption because the consumer load decreases from 90 kW to 40 kW, meaning that power excess is higher during that period.

The frequency behaviour is shown in Figure 13 using the per unit system, the frequency signal contains transients generated by the applied changes. They correspond to properly damped frequency increases for positive wind speed steps or negative load steps and vice versa.

The voltage RMS signal is shown in Figure 14 and contains transients related to the reactive power variations when system changes occur. The voltage control of the HP-WDPS is

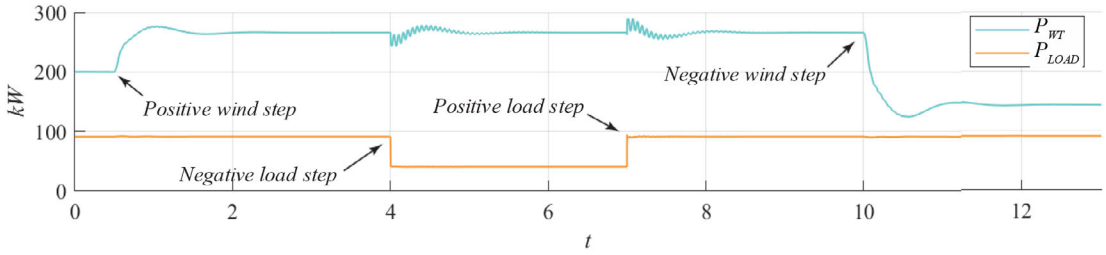

FIGURE 11 Active powers (kW) produced by the WTG and consumed by the loads for SOC = 95%.

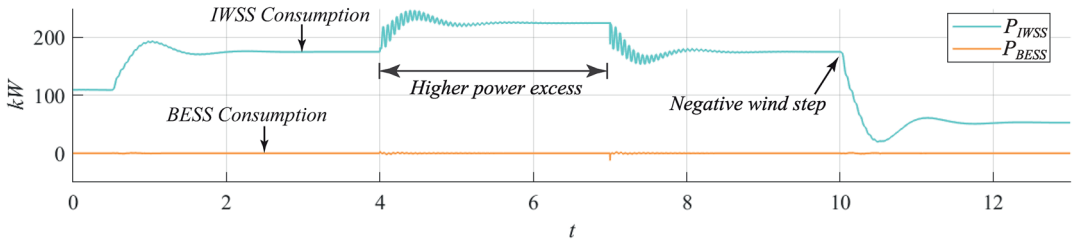

FIGURE 12 Active power (kW) exchanged by the BESS and consumed by the IWSS for SOC = 95%.

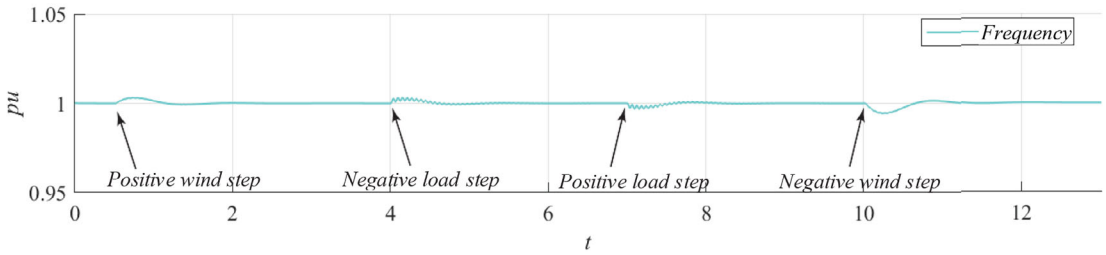

FIGURE 13 System frequency in per unit for SOC = 95%.

performed only by the AVR with the reactive power reference of the BESS and IWSS set to zero for energy efficiency. The consumer load variation has been modelled as an ideal step change of pure resistive value; the peak transient at $t = 4$ s is because of the limited dynamics of the AVR and the coupling between the active and reactive power in small networks, similar results can be found in [38]. However, the consumer load variations are never that abrupt and they are more progressive [39]. Another option is considering the reactive power capability of the power electronic converters, its analysis is left for another paper.

5.2 | Case SOC = 50%

For the case with SOC = 50%, the BESS can absorb the wind power excess and supply power to the consumer loads. At the beginning of the simulation, the BESS absorbs the active power excess and regulates the frequency as shown in Figure 15 to harness all the wind potential. This continues until the BESS has reached its nominal power of 150 kW from $t = 4$ s to $t = 7$ s, where the IWSS also consumes power and regulates the frequency. With the positive load step at $t = 7$ s, the IWSS starts consuming power and the BESS consumes the additional wind

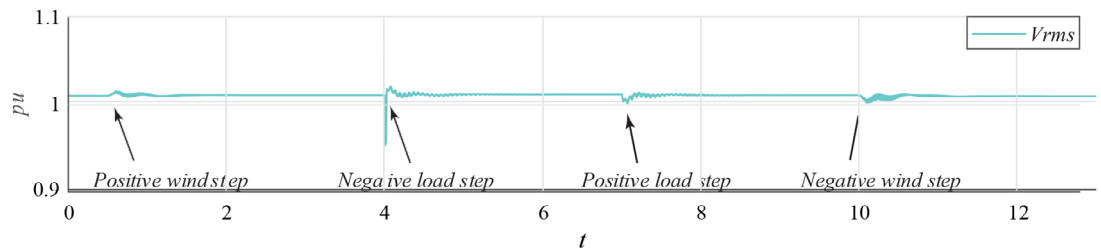

FIGURE 14 RMS voltage in per unit for SOC = 95%.

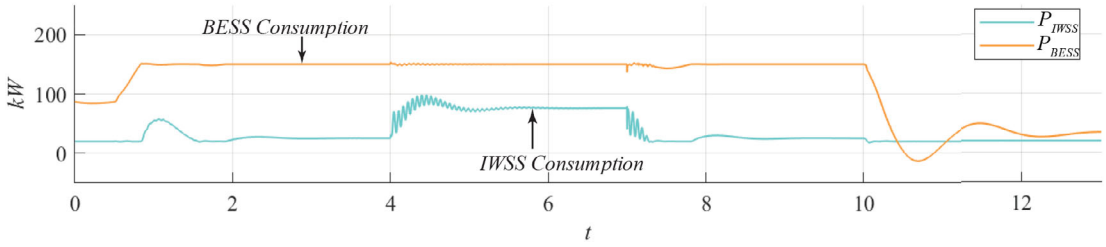

FIGURE 15 Active power (kW) exchanged by the BESS and consumed by the IWSS for SOC = 50%.

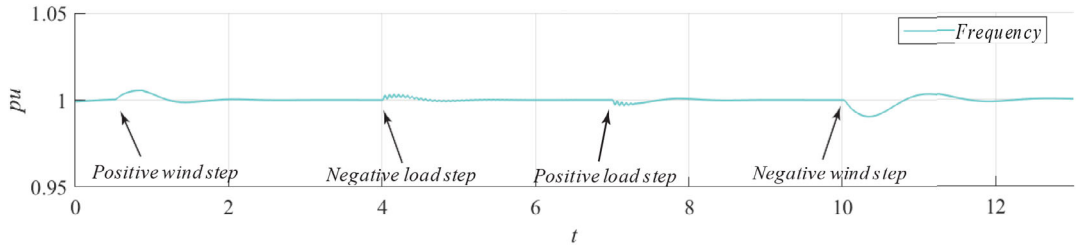

FIGURE 16 System frequency in per unit for SOC = 50%.

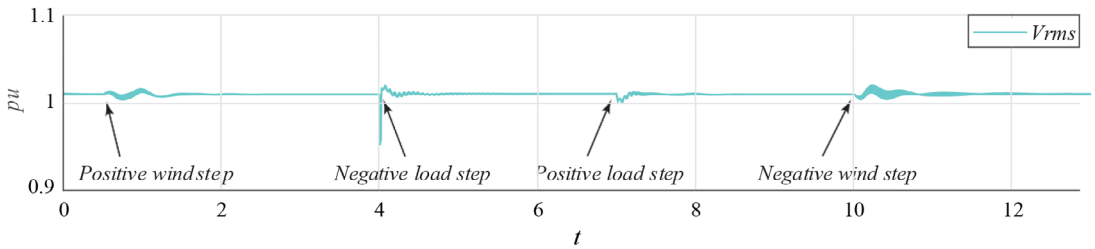

FIGURE 17 RMS voltage in per unit for SOC = 50%.

power and regulates the frequency. After the negative step in the wind speed at $t = 10$ s, the BESS carries out the frequency regulation by absorbing/supplying the necessary power to match the power production and consumption in the isolated system.

Figure 16 shows the system frequency, the transients resulting from the applied changes are very similar to those of the previous case. Also, the RMS voltage represented in per unit in Figure 17, shows similar behavior. This demonstrates that the system regulation is equally valid for the case of sharing the power output between the IWSS and the BESS.

The battery SOC, voltage V_{BAT} and current I_{BAT} in per unit are shown in Figure 18. In this case, I_{BAT} also follows the BESS power variations because of V_{BAT} remaining relatively constant. The small variations in V_{BAT} follow the current I_{BAT} as they are a consequence of the voltage drop due to the internal battery resistance.

5.3 | Case SOC = 10%

The last case presented has SOC = 10% with the BESS being able to store energy, but unable to supply power to the consumer loads. The wind speed is initially 10 m/s and changes to 11 m/s at $t = 0.5$ s, which increases the P_{WTG} from 200 kW to 265 kW. The wind power production of P_{WTG} falls to 25 kW when the wind speed decreases to 5 m/s at $t = 10$ s. The load power P_{CL} increases from an initial value of 40 kW up to 90 kW at $t = 4$ s and then decreases down to 40 kW at $t = 7$ s. These power variations for P_{WTG} and P_{CL} are shown in Figure 19.

The BESS and IWSS power are shown in Figure 20, the battery has the priority to absorb the wind-power excess and the IWSS only consumes power when the power ceiling of the BESS is reached; this happens after the increase in the wind speed at $t = 0.5$ s. The consumer load increases from 40 kW to 90 kW at $t = 4$ s and the IWSS is not required to absorb any wind power excess. Finally, at $t = 10$ s there is a huge decrease in the wind speed with a deficit in the power generation supplied to the consumer loads. With the SOC below the minimum to avoid deep battery discharge, the BESS is unable to supply any power to the consumer load. Under these circumstances, the system frequency decreases until collapsing unless the DG is ordered to start producing power by changing to the operation mode WD. Details on the transition from the WO operation mode to WD can be found in [40].

The frequency and voltage responses are shown in Figures 21 and 22, respectively. The variations follow the same patterns as

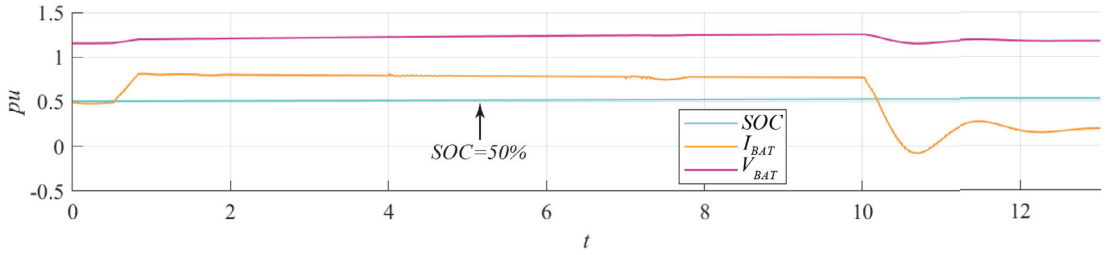

FIGURE 18 Battery measurement per unit: SOC, current and voltage for SOC = 50%.

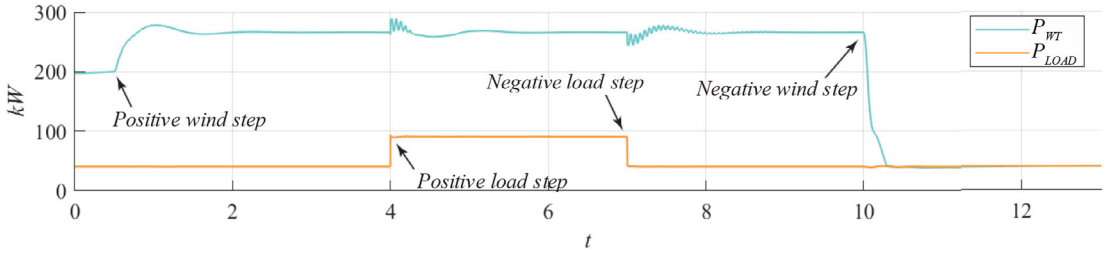

FIGURE 19 Active powers (kW) produced by the WTG and consumed by the loads for SOC = 10%.

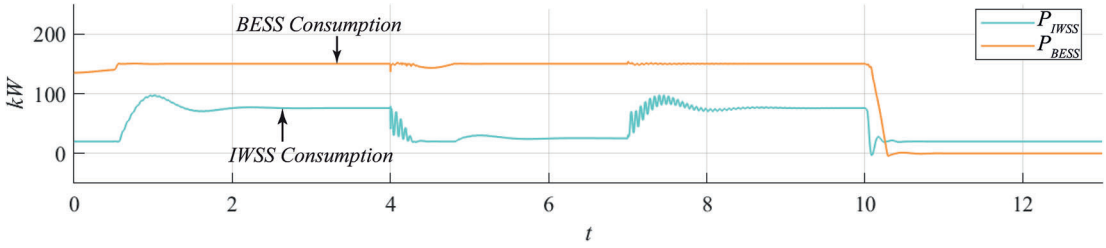

FIGURE 20 Active power (kW) exchanged by the BESS and consumed by the IWSS for SOC = 10%.

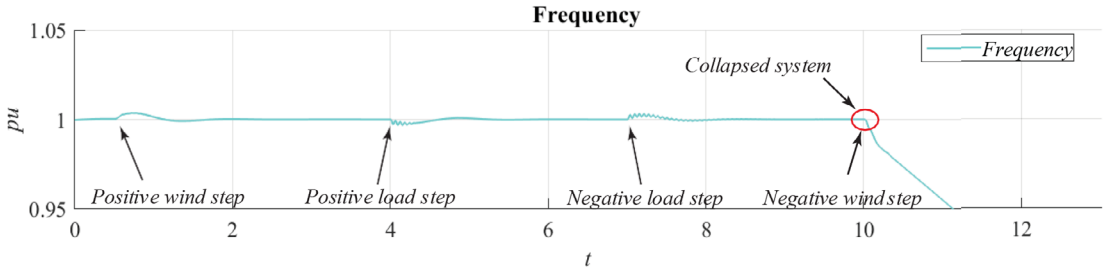

FIGURE 21 System frequency in per unit for SOC = 10%.

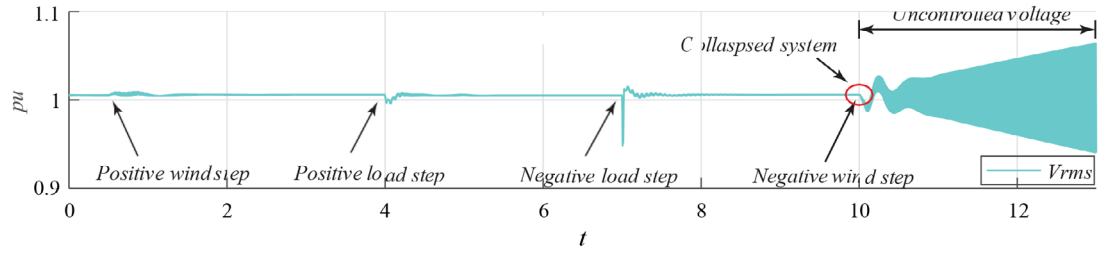

FIGURE 22 RMS voltage in per unit for SOC = 10%.

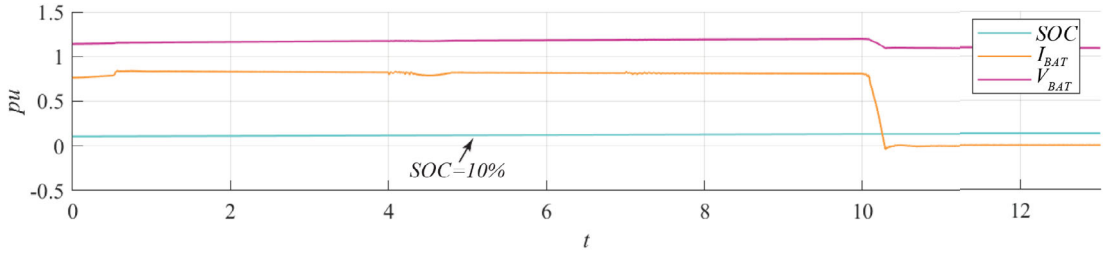

FIGURE 23 Battery measurement in per unit: SOC, current and voltage or SOC = 10%.

in the previous cases when the wind speed and consumer loads change abruptly. Figures 21 and 22 show the frequency (and eventually voltage) collapse when the battery is depleted and the wind speed does not result in sufficient power generation for feeding the consumer loads.

Finally, the battery SOC, voltage V_{BAT} and current I_{BAT} are shown in Figure 23 using the per unit system. The current I_{BAT} follows the BESS power and the voltage variations of V_{BAT} follow the I_{BAT}. After the drop in the wind speed at $t = 10$ s, there is a deficit in the active power. However, the battery current cannot become negative (discharge) because it is close to being depleted with SOC = 10% and the BESS is unable to supply electricity to the consumer loads.

6 | CONCLUSION

This article deals with HP-WDPSs, which combines WTGs and DGs and are able to work in the operation mode WO. The modelling of all the components present in the HP-WDPS under study as well as their controllers is thoroughly explained. The IWSS system uses a variable speed drive whose controller has the power consumption as the input reference so that it behaves as a controllable load. The BESS uses an efficient arrangement consisting of a three-phase full-bridge converter as the interface with the isolated grid and DAB for isolation and voltage level shifting. The BESS bidirectional converter absorbs the surplus power from wind power in periods of high wind speed and can generate power to the consumer load when wind speed is low. The proposed controller for the WO operation mode characteristic of the HP-WDPS uses a PI controller to regulate the frequency, which is tuned using the symmetrical optimum criterion. The proposed frequency controller establishes a sharing between the BESS and IWSS that gives full priority to the BESS to harness all the wind potential. The different SOCs in the battery are taken into account in the proposed algorithm. The different SOCs considered are BESS fully charged with no power absorption, BESS fully discharged and no power supplying and BESS allowed to absorb/supply power (20%<SOC<90%). Simulation results validate the proposed procedure with appropriate overall performance of the HP-WDPS that maintains the frequency and voltage values fully under control for different wind speed and load variations and different SOCs in the BESS.

AUTHOR CONTRIBUTIONS

José Luis Monroy-Morales: Conceptualization; data curation; formal analysis; investigation; methodology; project administration; resources; software; supervision; validation; visualization; writing—original draft; writing—review and editing. **Rafael Peña Alzola**: Conceptualization; data curation; formal analysis; funding acquisition; investigation; methodology; project administration; resources; software; supervision; validation; visualization; writing—original draft; writing—review and editing. **Rafael Sebastián-Fernández**: Methodology; project administration; supervision; writing—review and editing. **David Campos-Gaona**: Conceptualization; data curation; formal analysis; investigation; methodology; project administration; resources; software; supervision; validation; visualization; writing—review and editing. **Jerónimo Quesada Castellano**: Validation; writing—review and editing. **José L. Guardado**: Supervision; validation; writing—review and editing.

ACKNOWLEDGEMENTS

The authors would like to thank Pablo de Castro, Open Access Advocacy Librarian at the University of Strathclyde, for his assistance with the publication and Martin Macfadyen, PhD candidate at the University of Strathclyde, for proofreading the manuscript.

CONFLICT OF INTEREST STATEMENT

The authors declare no conflicts of interest.

DATA AVAILABILITY STATEMENT

Data available on request from the authors.

ORCID

Rafael Peña-Alzola https://orcid.org/0000-0002-2451-6779

REFERENCES

1. American Wind Energy Association: Wind/Diesel Systems Architecture Guidebook. American Wind Energy Association, Washington, DC (1991)
2. Vasileva, E.: A logical-probabilistic model for analysing the reliability of wind–diesel generator autonomous hybrid power system. In: 2022 14th Electrical Engineering Faculty Conference (BulEF), pp. 1–5. IEEE, Piscataway (2022)
3. Sebastián, R., García-Loro, F.: Review on wind diesel systems dynamic simulation. In: IECON 2019-45th Annual Conference of the IEEE Industrial Electronics Society, vol. 1, pp. 2489–2494. IEEE, Piscataway (2019)

4. Hunter, R., Elliot, G., (ed.): Designing a system. pp. 95–138. Cambridge University Press (1994)
5. Chen, H., Cong, TN., Yang, W., Tan, C., Li, Y., Ding, Y.: Progress in electrical energy storage system: A critical review. Prog. Nat. Sci. 19(3), 291–312 (2009)
6. Lu, C., Xu, H., Pan, X., Song, J.: Optimal sizing and control of battery energy storage system for peak load shaving. Energies 7(12), 8396–8410 (2014)
7. Wen, G., Hu, G., Hu, J., Shi, X., Chen, G.: Frequency regulation of source-grid-load systems: A compound control strategy. IEEE Trans. Ind. Inf. 12(1), 69–78 (2016)
8. Ahmad, P., Singh, N.: Optimal sizing of ess in a hybrid wind-diesel power system using nar and narx model. In: 2020 IEEE 7th Uttar Pradesh Section International Conference on Electrical, Electronics and Computer Engineering (UPCON), pp. 1–6. IEEE, Piscataway (2020)
9. Luo, X., Wang, J., Dooner, M., Clarke, J.: Overview of current development in electrical energy storage technologies and the application potential in power system operation. Appl. Energy 137, 511–536 (2015)
10. Xiong, R., Mu, H.: Accurate state of charge estimation for lithium-ion battery using dual uncsented kalman filters. In: 2017 Chinese Automation Congress (CAC), pp. 5484–5487. IEEE, Piscataway (2017)
11. Keshan, H., Thornburg, J., Ustun, T.S.: Comparison of lead-acid and lithium ion batteries for stationary storage in off-grid energy systems. In: 4th IET Clean Energy and Technology Conference (CEAT 2016), pp. 1–7. IET, Stevenage (2016)
12. Sebastián, R., Quesada, J.: Coordinated control of a battery energy storage and a dump load in an autonomous wind power system. In: 2020 IEEE International Conference on Environment and Electrical Engineering and 2020 IEEE Industrial and Commercial Power Systems Europe (EEEIC/I&CPS Europe), pp. 1–6. IEEE, Piscataway (2020)
13. Sebastián, R., Peña-Alzola, R.: Flywheel energy storage and dump load to control the active power excess in a wind diesel power system. Energies 13(8), 2029 (2020)
14. Sebastián, R.: Battery energy storage for increasing stability and reliability of an isolated wind diesel power system. IET Renewable Power Gener. 11(2), 296–303 (2017)
15. Tan, N.M.L., Abe, T., Akagi, H.: Design and performance of a bidirectional isolated dc–dc converter for a battery energy storage system. IEEE Trans. Power Electron. 27(3), 1237–1248 (2012)
16. Tan, N.M.L., Abe, T., Akagi, H.: Topology and application of bidirectional isolated dc-dc converters. In: 8th International Conference on Power Electronics - ECCE Asia, pp. 1039–1046. IEEE, Piscataway (2011)
17. Teodorescu, R., Liserre, M., Rodriguez, P.: Grid converters for photovoltaic and wind power systems. John Wiley & Sons, Chichester (2011)
18. Al-Khalifah, M., McMillan, G.: Control valve versus variable-speed drive for flow control. ISA Autom. Week 60(4), 42–46 (2012)
19. Beyer, H.G., Degner, T., Gabler, H.: Operational behaviour of wind diesel systems incorporating short-term storage: An analysis via simulation calculations. Solar Energy 54(6), 429–439 (1995)
20. Hansen, A.D., Iov, F., Sørensen, P., Cutululis, N., Jauch, C., Blaabjerg, F., et al.: Dynamic Wind Turbine Models in Power System Simulation Tool DIgSILENT. Contract ENS-1363/04-0008; ENS-33030-0003; ENS-1363/01-0013. Risø National Laboratory, Roskilde (2007)
21. Kamal, E., Koutb, M., Sobaih, A.A., Abozalam, B.: An intelligent maximum power extraction algorithm for hybrid wind–diesel-storage system. Int. J. Electric Power Energy Syst. 32(3), 170–177 (2010)
22. Haruni, A.M.O., Gargoom, A., Haque, M.E., Negnevitsky, M.: Dynamic operation and control of a hybrid wind-diesel stand alone power systems. In: 2010 Twenty-Fifth Annual IEEE Applied Power Electronics Conference and Exposition (APEC), pp. 162–169. IEEE, Piscataway (2010)
23. Lukasievicz, T., Oliveira, R., Torrico, C.: A control approach and supplementary controllers for a stand-alone system with predominance of wind generation. Energies 11(2), 411 (2018)
24. Tiwari, S.K., Singh, B., Goel, P.K.: Control of wind–diesel hybrid system with bess for optimal operation. IEEE Trans. Ind. Appl. 55(2), 1863–1872 (2019)
25. Amenedo, J.L.R., Gómez, S.A., Díaz, J.C.B., Gómez, D.A., Guerra, T.A.: Sistemas eólicos de producción de energía eléctrica. Rueda (2003)
26. Margaris, I.D., Papathanassiou, S.A., Hatziargyriou, N.D., Hansen, A.D., Sorensen, P.: Frequency control in autonomous power systems with high wind power penetration. IEEE Trans. Sustainable Energy 3(2), 189–199 (2012)
27. Wilches-Bernal, F., Darbali-Zamora, R., Naughton, B.T., Flicker, J.D.: Model characterization and frequency regulation in wind-diesel hybrid microgrids. In: 2022 North American Power Symposium (NAPS), pp. 1–5. IEEE, Piscataway (2022)
28. MathWorks. Simscape ™ fluids ™user's guide (2020)
29. Kim, S.H.: Electric Motor Control: DC, AC, and BLDC Motors. Elsevier Science, Amsterdam (2017)
30. Keshan, H., Thornburg, J., Ustun, T.S.: Comparison of lead-acid and lithium ion batteries for stationary storage in off-grid energy systems. In: 4th IET Clean Energy and Technology Conference (CEAT 2016), pp. 1–7. IET, Stevenage (2016)
31. Dufo-López, R., Cortés-Arcos, T., Artal-Sevil, J.S., Bernal-Agustín, J.L.: Comparison of lead-acid and li-ion batteries lifetime prediction models in stand-alone photovoltaic systems. Appl. Sci. 11(3), 1099 (2021)
32. Podder, S., Khan, M.Z.R.: Comparison of lead acid and li-ion battery in solar home system of bangladesh. In: 2016 5th International Conference on Informatics, Electronics and Vision (ICIEV), pp. 434–438. IEEE, Piscataway (2016)
33. De Doncker, R.W.A.A., Divan, D.M., Kheraluwala, M.H.: A three-phase soft-switched high-power-density dc/dc converter for high-power applications. IEEE Trans. Ind. Appl. 27(1), 63–73 (1991)
34. MathWorks: Simscape electrical/specialized power systems (2020)
35. Harnefors, L., Nee, H.: A general algorithm for speed and position estimation of ac motors. IEEE Trans. Ind. Electron. 47(1), 77–83 (2000)
36. Umland, J.W., Safiuddin, M.: Magnitude and symmetric optimum criterion for the design of linear control systems: what is it and how does it compare with the others? IEEE Trans. Ind. Appl. 26(3), 489–497 (1990)
37. Leonhard, W.: Control of Electrical Drives. Power Systems. Springer Berlin Heidelberg (2001)
38. Janssen, N.T., Wies, R.W., Peterson, R.A.: Frequency regulation by distributed secondary loads on islanded wind-powered microgrids. IEEE Trans. Sustainable Energy 7(3), 1028–1035 (2016)
39. Bindner, H., Universitet, D.T.: Isolated Systems with Wind Power: Results of Measurements in Egypt. Risø-R. Risø DTU - National Laboratory for Sustainable Energy (2001)
40. Sebastián, R.: Smooth transition from wind only to wind diesel mode in an autonomous wind diesel system with a battery-based energy storage system. Renew. Energy 33(3), 454–466 (2008)

How to cite this article: Monroy-Morales, J.L., Peña-Alzola, R., Sebastián-Fernández, R., Campos-Gaona, D., Castellano, J.Q., Guardado, J.L.: Frequency control in an isolated wind-diesel hybrid system with energy storage and an irrigation water supply system. IET Renew. Power Gener. 1–15 (2024). https://doi.org/10.1049/rpg2.12950